

## CELLULAR ASSOCIATION, INTRACELLULAR DISTRIBUTION, AND EFFLUX OF AURANOFIN VIA SEQUENTIAL LIGAND EXCHANGE REACTIONS

ROSANNE M. SNYDER,\*†§ CHRISTOPHER K. MIRABELLI‡§ and STANLEY T. CROOKE‡§

‡ Department of Molecular Pharmacology, Smith Kline & French Laboratories, Philadelphia, PA 19101; and § Department of Pharmacology, School of Medicine, University of Pennsylvania, Philadelphia, PA 19104, U.S.A.

(Received 14 May 1985; accepted 15 August 1985)

**Abstract**—Auranofin (AF), an orally active, antiarthritic agent, modulates the functional activities of macrophages *in vivo* and *in vitro*. To better understand the molecular mechanism of action of auranofin with macrophages we have investigated its cellular association, intracellular distribution, and efflux with RAW 264.7 cells using auranofin radiolabeled within the triethylphosphine ( $\text{Et}_3\text{P}$ ) [ $^3\text{H}$ ], the gold [ $^{195}\text{Au}$ ] or the tetraacetylthioglucose (TATG) [ $^{14}\text{C}$ ] moieties of the molecule. Evaluation of the effects of auranofin on RAW 264.7 cells demonstrates that (1) cellular association of this compound was concentration, time and temperature dependent; (2) cellular association of AF was inhibited by *N*-ethylmaleimide but not by 2,4-dinitrophenol and NaF; (3) cellular association and uptake of Au and  $\text{Et}_3\text{P}$  into cells was reduced when the drug was preincubated with increasing concentrations of fetal calf serum and albumin; (4) no tetraacetylthioglucose from the auranofin molecule became cell associated whereas the Au and  $\text{Et}_3\text{P}$  moieties were internalized and distributed between the nuclear, cytosolic and membrane fractions of cells; and (5) efflux of Au and  $\text{Et}_3\text{P}$  from RAW 264.7 cells was time and temperature dependent. Based on these data we propose a model, a sequential ligand exchange process, that describes the molecular interactions of auranofin and possibly other gold compounds with these cells.

Gold complexes have been employed as therapeutic agents for rheumatoid arthritis since the early part of the 20th century [1-4]. The most commonly used drugs are water soluble, parenterally administered, gold(I) thiolates such as gold sodium thiomalate (Myochrysine) and gold sodium thioglucose (Solganol) [2, 3]. Even though these compounds have a multiplicity of effects (e.g. inhibition of enzymes, interaction with the immune system) in various experimental systems and induce remission of disease activity *in vivo* [3, 4], little is known concerning the molecular mechanisms of association and uptake into cells or cellular effects.

Auranofin (AF), || [(2,3,4,6-tetra-*O*-acetyl-1-thio- $\beta$ -D-glucopyranosato-S)(triethylphosphine)gold(I)], is an orally active antiarthritic chrysotherapeutic agent [5, 6] (Fig. 1). Although its mechanism of action is unknown, recent evidence suggests that a primary therapeutic target is the macrophage, a cell that plays a critical role in the initiation and maintenance of chronic rheumatoid synovitis [7-9].

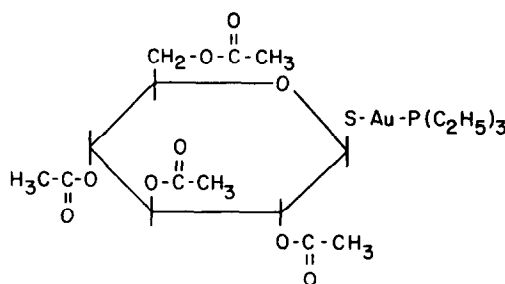


Fig. 1. Structure of auranofin [(2,3,4,6-tetra-*O*-acetyl-1-thio- $\beta$ -D-glucopyranosato-S)(triethylphosphine) gold(I)]. The compound was labeled with [ $^{195}\text{Au}$ ], [ $^3\text{H}$ ] and [ $^{14}\text{C}$ ] at the sites described in Materials and Methods.

Auranofin modulates a number of macrophage functions *in vitro* and *in vivo*, including chemotaxis, phagocytosis, antigen presentation, and  $\text{F}_c$  and  $\text{C}_3$  receptor expression [7, 9]. In addition, monocytes preincubated with the drug are unable to support mitogen-induced proliferation of T-lymphocytes [7, 9-11].

In patients and experimental animals that were administered parenteral gold compounds, gold was distributed and bound to serum proteins but was primarily sequestered in reticulo-endothelial organs that contained the greatest number of mononuclear phagocytes [12, 13]. Electron microscopic and electron probe X-ray analyses have localized gold in aurosomes, lysosomes or lysosome-like organelles, within these phagocytic cells [12-15]. Few studies have examined in detail the subcellular distribution of parenteral gold salts and none to date have exam-

\* R. M. S. is a predoctoral trainee supported by the University of Pennsylvania, Department of Pharmacology.

† To whom reprint requests should be sent: R. M. Snyder, Smith Kline & French Laboratories, L-511, 1500 Spring Garden St., Philadelphia, PA 19101.

|| Abbreviations: AF, auranofin [(2,3,4,6-tetra-*O*-acetyl-1-thio- $\beta$ -D-glucopyranosato-S)(triethylphosphine)gold(I)];  $\text{Et}_3\text{P}$ , triethylphosphine; TATG, tetraacetylthioglucose; FCS, fetal calf serum; DMEM, Dulbecco's low glucose minimal essential medium; NEM, *N*-ethylmaleimide; DNP, 2,4-dinitrophenol; PBS, phosphate-buffered saline; and MØ, macrophages.

ined the intracellular distribution of auranofin. However, differential centrifugation and electron microscopic analyses suggested that gold from gold salts was present in nuclear, cytosolic, mitochondrial and lysosomal fractions of rat liver and kidney cortex cells [12, 14, 16].

To better understand auranofin's mechanism of action and interaction with macrophages, we have examined its effects on RAW 264.7 macrophage-like cells [17]. In this report we describe the cellular association of radiolabeled auranofin and its intracellular distribution and efflux from RAW 264.7 cells. Results of our studies allow us to propose a model, a sequential thiol exchange process, that describes the molecular interactions of auranofin responsible for its cellular uptake, distribution, and efflux.

#### MATERIALS AND METHODS

**Materials.** [ $^{195}\text{Au}$ ]Auranofin (2.0 mCi/mmol) was obtained from Dupont New England Nuclear. [ $^{14}\text{C}$ ]Auranofin (10.8 mCi/mmol), uniformly labeled on the carbons within the glucose ring, and [ $^3\text{H}$ ]auranofin (21 mCi/mmol), uniformly labeled in the triethylphosphine moiety of the molecule, were synthesized by the Radiochemistry Department at Smith Kline & French Laboratories. Pentex reagent grade bovine albumin, fraction V, was obtained from Miles Scientific, and fetal calf serum (FCS) was purchased from Grand Island Biological. *N*-Ethylmaleimide was obtained from Baker. All other chemicals were obtained from the Sigma Chemical Co.

**Cell culture techniques.** RAW 264.7 cells, a murine macrophage-like cell line obtained from the American Type Culture collection (ATCC TIB 71), were grown in monolayer in DMEM containing 10% FCS in a 5%  $\text{CO}_2$  humidified incubator at 37°.

**Cell association of radiolabeled auranofin.** Asynchronous, confluent populations of RAW 264.7 cells were scraped from T-150 mm flasks and resuspended in fresh DMEM to achieve a final concentration of  $1.2 \times 10^6$  cells/ml. Medium containing 100  $\mu\text{l}$  of [ $^{195}\text{Au}$ ]-, [ $^{14}\text{C}$ ]- or [ $^3\text{H}$ ]-labeled auranofin was added to 900  $\mu\text{l}$  of cell suspension. Cells and the radiolabeled compound were incubated under conditions described in Results. The reactions were stopped by placing the tubes on ice and centrifuging the reaction mixture at 4° in a Beckman Tabletop Centrifuge for 5 min at 3000 rpm. After centrifugation, the supernatant fraction was removed from the tubes. Both supernatant fraction and cell pellet were placed in scintillation vials, and radioactivity was determined in either a Beckman Gamma 8000 Counter ([ $^{195}\text{Au}$ ]AF) or a Beckman Liquid Scintillation Counter ([ $^{14}\text{C}$ ]- and [ $^3\text{H}$ ]AF).

Cells ( $1 \times 10^6$  cells/ml) were also treated with increasing concentrations of DNP, NEM, and NaF for 5, 30 and 60 min respectively. The reactions were stopped by centrifuging the reaction mixture at 4° for 5 min at 3000 rpm. After centrifugation, the supernatant fraction was removed from the tubes and the cell pellets were washed three times with ice-cold PBS. After recentrifugation for 5 min at 4° at 3000 rpm, the supernatant fraction was again

removed from the centrifuge tubes. The cells were then resuspended in 900  $\mu\text{l}$  of fresh DMEM and 100  $\mu\text{l}$  [ $^{195}\text{Au}$ ]AF (5  $\mu\text{M}$ ) and incubated for 10 min at 37° in a shaking water bath. The reactions were stopped and radioactivity was determined as described in the previous section.

**Determination of initial rates of [ $^{195}\text{Au}$ ]AF cell association.** The rate of cellular association of auranofin was treated as a simple pseudo-first order process with respect to cellular sulfhydryl groups, a treatment which seems reasonable in view of the estimated sulfhydryl group concentration in cellular membranes and the large excess of auranofin used. The experimental data were fit by a standard multiple parameter, least squares analysis to a semilogarithmic plot which provides pseudo-first order rate constants directly from the slope of the resulting linear expression.

**Subcellular fractionation of radiolabeled AF-treated RAW 264.7 cells.** RAW 264.7 cells were fractionated into crude nuclear, cytosolic and crude membrane fractions. Radiolabeled AF was incubated with  $1 \times 10^6$  cells over a 60-min period at 37°, centrifuged at 3000 rpm for 5 min at 4°, and the supernatant fraction removed. The cell pellet was washed once with ice-cold PBS, recentrifuged at 3000 rpm for 5 min, and the supernatant fraction again removed. Cells were hypotonically lysed on ice in 1.2 ml of cold 1 mM  $\text{NaHCO}_3$  by periodic, gentle trituration over a 60-min period. Efficiency of lysis was assessed by microscopic examination. After lysis, a crude nuclear fraction containing approximately 85% nuclei, 15% whole cells, and some cellular debris was obtained by centrifuging the cellular lysate at 1000 rpm for 7 min. The supernatant fraction was then transferred to Beckman 11  $\times$  34 mm polycarbonate centrifuge tubes and centrifuged in a Beckman TL-100 tabletop ultracentrifuge at 45,000 rpm for 45 min at 4°. After centrifugation, the supernatant (cytosolic fraction) was removed, the pellet (crude membrane) washed once with cold PBS, and the mixture recentrifuged at 45,000 rpm for 45 min. The crude nuclear, cytosolic and crude membrane fractions were placed in scintillation vials and their radioactivity was determined.

**Efflux of radiolabeled auranofin.** Radiolabeled AF (5  $\mu\text{M}$ ) was incubated with  $1 \times 10^6$  macrophages for 20 min in a 37° shaker water bath (New Brunswick Scientific). The cells were then centrifuged at 3000 rpm  $\times$  5 min, washed once with PBS, recentrifuged, and the supernatant removed. The cells were resuspended in 1.0 ml DMEM. After a second incubation at either 4° or 37° for specified times, the reaction mixture was centrifuged at 3000 rpm for 5 min and the supernatant fraction removed. The cell pellet and supernatant fraction were transferred to scintillation vials, and radioactivity was determined in either a Beckman Gamma or Scintillation Counter.

#### RESULTS

**Association of radiolabeled AF with RAW 264.7 cells.** The association of radiolabeled AF with macrophages was measured as described in Materials and Methods. The amount of cell-associated [ $^{195}\text{Au}$ ] was linearly proportional to the concentration of AF up

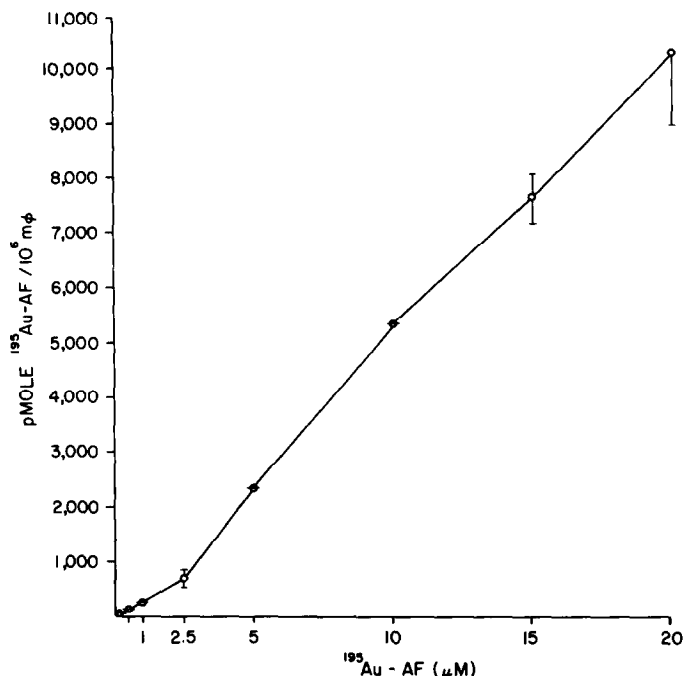


Fig. 2. Concentration-dependent cell association of [ $^{195}\text{Au}$ ]. Experimental procedures are as described in Materials and Methods. The values shown are means and standard deviations derived from two separate experiments performed in duplicate.

to a 20  $\mu\text{M}$  concentration of the drug (Fig. 2). Under the experimental conditions used in these studies, incubation of the cells with concentrations of AF greater than 20  $\mu\text{M}$  produced significant cell lysis.

Figure 3 shows the time course of association of [ $^{195}\text{Au}$ ]-, [ $^3\text{H}$ ]Et $_3\text{P}$ - and [ $^{14}\text{C}$ ]TATG-labeled AF. The cell-associated [ $^{195}\text{Au}$ ] and [ $^3\text{H}$ ]Et $_3\text{P}$  radiolabels increased as a function of time for 10 min and plateaued between 10 and 30 min. The amount of

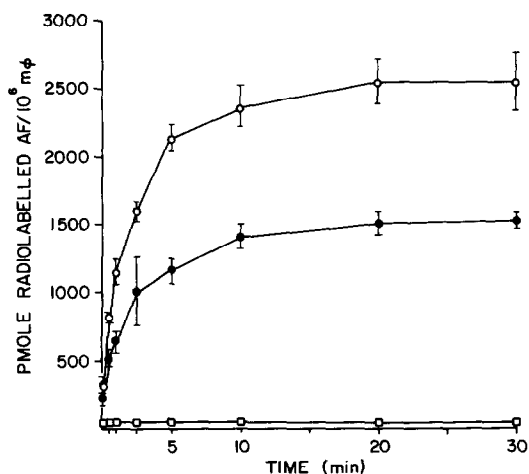


Fig. 3. Cell association of auranofin radiolabeled in three sites as a function of time. Procedures are as described in Materials and Methods. Values shown are means and standard deviations from two separate experiments performed in duplicate for each of the radioactively labeled compounds. Key: (○—○) [ $^{195}\text{Au}$ ]; (●—●) [ $^3\text{H}$ ]Et $_3\text{P}$ ; and (□—□) [ $^{14}\text{C}$ ]TATG.

radiolabel in the cell pellet decreased between 30 and 60 min, perhaps due to cytotoxic effects of the drug resulting in cell lysis and death. A constant, small amount of [ $^{14}\text{C}$ ] from [ $^{14}\text{C}$ ]TATG-AF, less than 1% of the total input radioactivity, associated with cells during the 60-min reaction period. At the earliest time points, the stoichiometry of [ $^{195}\text{Au}$ ] and [ $^3\text{H}$ ]Et $_3\text{P}$  association was approximately 1:1. This ratio changed as the time of incubation increased and more [ $^{195}\text{Au}$ ] than [ $^3\text{H}$ ]Et $_3\text{P}$  was associated with cells at time points between 2 and 60 min. During the time at which equilibrium existed for each radiolabeled compound, 10–30 min, the molar ratio of [ $^{195}\text{Au}$ ] to [ $^3\text{H}$ ]Et $_3\text{P}$  was approximately 2:1.

Cellular association and uptake of [ $^{195}\text{Au}$ ] from radiolabeled AF as a function of time was temperature dependent over the range of temperatures studied (Fig. 4). The percent cell association at equilibrium was equivalent at all temperatures except 4°. At 4°, equilibrium was not achieved even after a 90-min incubation (data not shown). At 15°, 18° and 22° (18° and 22° data not shown), the [ $^{195}\text{Au}$ ] associated with the cell pellet increased linearly up to 60 min and plateaued between 60 and 90 min. At 37° cell association was linear up to 10 min, but decreased after 30 min, presumably due to cell death. The cytotoxic effects of auranofin are also temperature dependent [18]. For example, a 90-min incubation with 5  $\mu\text{M}$  auranofin at 37° resulted in an approximate 30% reduction in the number of cells, while a similar incubation at lower temperatures caused no diminution in cell number. The data in Fig. 5 demonstrate that the initial rates of cell association increased as the temperature increased.

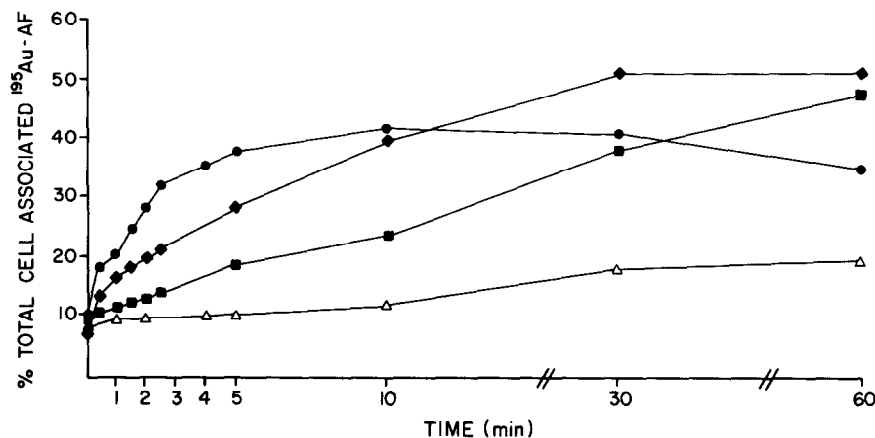


Fig. 4. Effects of temperature on cell association of [ $^{195}\text{Au}$ ] over time. The percent of total input radioactivity associated with cells was determined at various times and temperatures as described in Materials and Methods. Additional studies were performed at 18°, 22° and 30° (these data were not included to simplify the figure). The values shown are means from three separate experiments performed in duplicate. The standard deviations were less than 10%. Key: ( $\triangle$ — $\triangle$ ) 4°; ( $\blacksquare$ — $\blacksquare$ ) 15°; ( $\blacklozenge$ — $\blacklozenge$ ) 27° and ( $\bullet$ — $\bullet$ ) 37°.

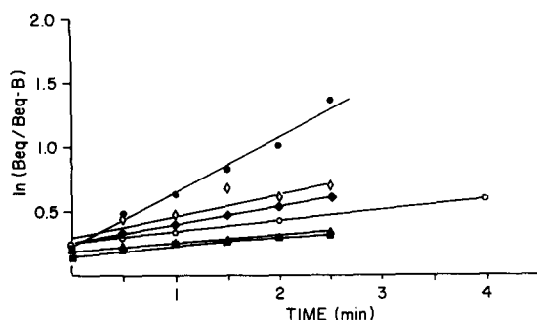


Fig. 5. Initial rates of association with cells of [ $^{195}\text{Au}$ ] as a function of temperature. The natural log of cell-associated [ $^{195}\text{Au}$ ] at equilibrium, derived from the cell-associated [ $^{195}\text{Au}$ ] at each time, is plotted versus time. The values are derived from the experiments shown in Fig. 4. Key: ( $\blacksquare$ — $\blacksquare$ ) 15°; ( $\blacktriangle$ — $\blacktriangle$ ) 18°; ( $\circ$ — $\circ$ ) 22°; ( $\blacklozenge$ — $\blacklozenge$ ) 27°; ( $\diamond$ — $\diamond$ ) 30° and ( $\bullet$ — $\bullet$ ) 37°.

Table 1. Effects of NEM, DNP and NaF pretreatment on cellular association of auranofin

Drug concn ( $\mu\text{M}$ )	% Total cell-associated [ $^{195}\text{Au}$ ]		
	NEM	DNP	NaF
0	100	100	100
0.1	96 $\pm$ 7	107 $\pm$ 5	
1	94 $\pm$ 4	98 $\pm$ 7	
10	53 $\pm$ 5	97 $\pm$ 8	103 $\pm$ 0.6
100	24 $\pm$ 3	93 $\pm$ 12	102 $\pm$ 4
1000	15 $\pm$ 2		106 $\pm$ 7
10,000			104 $\pm$ 1

RAW 264.7 cells ( $1 \times 10^6$  cells/ml) were pretreated with DNP, NEM and NaF for 5, 30 and 60 min, respectively, and washed three times with PBS. The cells were then treated with [ $^{195}\text{Au}$ ]AF (5  $\mu\text{M}$ ) for 10 min; the reaction was stopped and radioactivity determined as described in Materials and Methods. Values represent percent total cell-associated [ $^{195}\text{Au}$ ]. One hundred percent (the amount of [ $^{195}\text{Au}$ ] incorporated into cells in the absence of inhibitor) is equivalent to 2400 pmoles [ $^{195}\text{Au}$ ] per  $1 \times 10^6$  cells.

*Cellular association of [ $^{195}\text{Au}$ ]AF after pretreatment with NEM, DNP and NaF.* The data in Table 1 show that association of [ $^{195}\text{Au}$ ] from radiolabeled AF was inhibited by a 30-min pretreatment of cells with NEM, a sulfhydryl alkylating reagent. Significant inhibition of cell association was observed at the higher concentrations of the compound, with 1000  $\mu\text{M}$  NEM resulting in an 85% reduction in [ $^{195}\text{Au}$ ] association relative to control. Cells pretreated for 5 min with DNP, an oxidative phosphorylation uncoupler, showed no significant reduction of [ $^{195}\text{Au}$ ] cell association relative to control at any concentrations tested. The concentrations of DNP used in our studies were similar to those reported to disrupt mitochondrial function significantly [19–21]. Cells pretreated for 60 min with NaF, a compound that inhibits phagocytosis and pinocytosis [22], also had no effect upon [ $^{195}\text{Au}$ ] cell association.

*Effect of fetal calf serum on [ $^{195}\text{Au}$ ]AF cellular association.* Auranofin has been reported to bind to serum proteins, particularly serum albumin, both *in vivo* and *in vitro*, presumably through interactions with the free cysteine-34 sulfhydryl group [3, 4, 23]. FCS also reduced the cytotoxic potency of auranofin against B16 cells in a clonogenic assay and resulted in a 2- to 3-fold decrease in B16 cell-associated gold [18]. Figure 6 shows the effect of preincubating 5  $\mu\text{M}$  [ $^{195}\text{Au}$ ]AF with increasing concentrations of FCS on [ $^{195}\text{Au}$ ] cell association. Inclusion of FCS reduced cellular association of the label in a concentration-dependent manner with 10% FCS resulting in a 20-fold reduction in cell-associated gold relative to control after 60 min. In a separate experiment, we determined by toluene extraction [18] that gold incubated with 10% FCS resulted in approximately 100% of the gold becoming protein bound. As seen in our data, even when cells were incubated with the drug and 10% FCS, we found that 5% of the [ $^{195}\text{Au}$ ] label became cell associated. Equimolar amounts of FCS and albumin resulted in similar inhibition of [ $^{195}\text{Au}$ ]

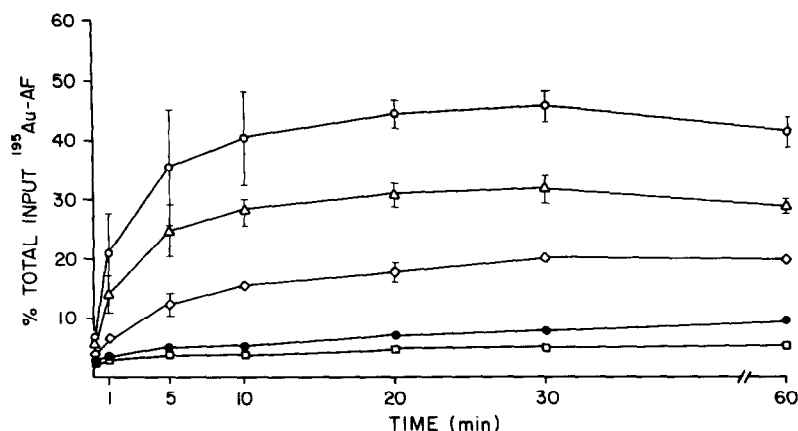


Fig. 6. Effects of FCS on the cell association of 5  $\mu\text{M}$  [ $^{195}\text{Au}$ ]AF. Experimental procedures are as described in Materials and Methods. The values are means and standard deviations from two separate experiments performed in duplicate. Key: (○—○) control; (△—△) 1% FCS; (◇—◇) 2% FCS; (●—●) 5% FCS and (□—□) 10% FCS.

cell association (data not shown). Increasing concentrations of FCS also reduced the amount of [ $^3\text{H}$ ]Et $_3$ P radiolabel derived from auranofin associated with the cell pellet (data not shown).

**Subcellular localization of radiolabeled auranofin.** The intracellular distribution of radiolabeled auranofin with RAW 264.7 cells was studied as described in Materials and Methods. The distribution of [ $^{195}\text{Au}$ ] in the nuclear, cytosolic and crude membrane fractions remained constant with increasing concentrations of the drug (Fig. 7), but varied with time when 5  $\mu\text{M}$  radiolabeled drug was incubated with cells up to 60 min (Fig. 8 A, B and C). As was seen previously (Fig. 2), no [ $^{14}\text{C}$ ] from [ $^{14}\text{C}$ ]TATG-AF associated with, and was distributed in, these cells. In the nuclear fraction, the amount of [ $^{195}\text{Au}$ ] was relatively constant while, over time, the nuclear-associated [ $^3\text{H}$ ]Et $_3$ P increased. The early appearance of [ $^{195}\text{Au}$ ] in the nucleus may result from normal cellular metabolism of the Au-Et $_3$ P and sequential

shuttling of the gold to the nucleus. However, after continued exposure to the drug, these metabolizing systems may be damaged and increasing amounts of Au-Et $_3$ P may gradually accumulate at these sites. However, other explanations, e.g. nuclear accumulation of Et $_3$ P, cannot be excluded. Our data are consistent with the subcellular localization and autoradiographic studies from other laboratories reporting gold association with nuclei and nuclear membranes in rat liver, kidney and rabbit macrophages after administration of gold sodium thiomalate i.v. [3, 12, 14]. Furthermore, we demonstrate the presence of [ $^3\text{H}$ ]Et $_3$ P in the nuclear fraction and that cell association and subcellular distribution of [ $^{195}\text{Au}$ ] and [ $^3\text{H}$ ]Et $_3$ P may be partially independent post 2 min.

The distribution of both the [ $^{195}\text{Au}$ ] and [ $^3\text{H}$ ]Et $_3$ P moieties into the cytosolic fraction increased with time, reaching a plateau after 5–10 min (Fig. 8B). At short time points, the ratio of [ $^{195}\text{Au}$ ] and [ $^3\text{H}$ ]Et $_3$ P

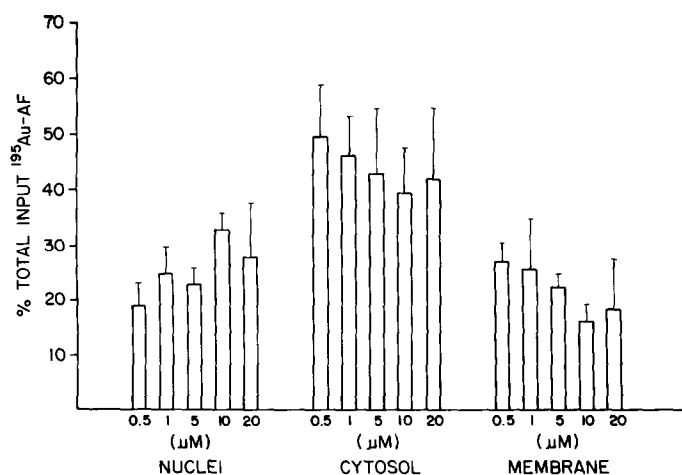


Fig. 7. Concentration-dependent association of [ $^{195}\text{Au}$ ] with nuclear, cytosolic and membrane fractions of cells. Cells were treated with increasing concentrations of [ $^{195}\text{Au}$ ]AF for 30 min at 37°. The values shown are means and standard deviations of two separate experiments performed in duplicate.

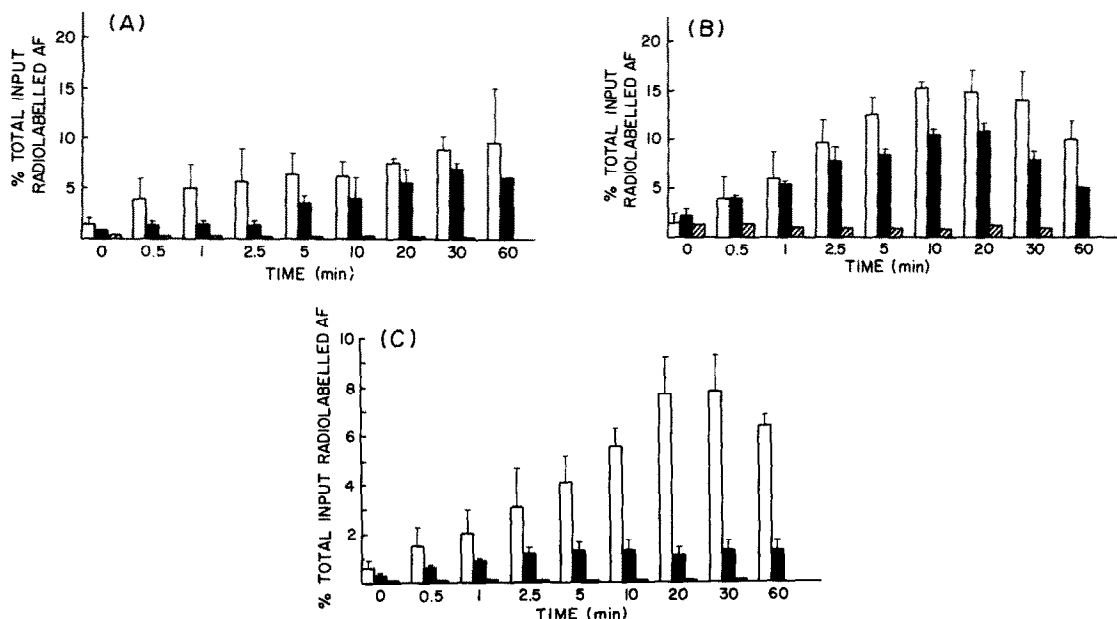


Fig. 8. Intracellular distribution of auranofin radiolabel as a function of time. Experimental procedures are as described in Materials and Methods. Figure 8A represents radioactivity associated with crude nuclei; 8B radioactivity present in the cytosolic fraction; and 8C radioactivity present in the crude membrane fraction. The values shown are means and standard deviations from two separate experiments in duplicate for each of the radioactive compounds. Key: ( $\square$ )  $[^{195}\text{Au}]\text{AF}$ ; ( $\blacksquare$ )  $[^3\text{H}]\text{Et}_3\text{P-AF}$ ; and ( $\square$ )  $[^{14}\text{C}]\text{TATG-AF}$ .

in cytosol was approximately 1:1. Although, with increasing time, more  $[^{195}\text{Au}]$  than  $[^3\text{H}]\text{Et}_3\text{P}$  was found in the cytosol, the pattern of cytosolic distribution was similar. Essentially no  $[^{14}\text{C}]\text{TATG}$  was present in the cytosol. In the crude membrane fraction, the amount of  $[^3\text{H}]\text{Et}_3\text{P}$  found was relatively constant as a function of time. In contrast,  $[^{195}\text{Au}]$  increased with time. Again, no significant  $[^{14}\text{C}]\text{TATG}$  was observed in the membrane fraction. Consequently, the 2-fold greater amount of  $[^{195}\text{Au}]$  compared to  $[^3\text{H}]\text{Et}_3\text{P}$  in the cellular pellet is largely due to differences in the amounts of each associated with membranes.

**Efflux of radiolabeled auranofin.** As shown in Fig. 9, efflux by auranofin increased as a function of incubation time in fresh medium. Cells preincubated with  $5\ \mu\text{M}$  radiolabeled drug retained twice as much  $[^{195}\text{Au}]$  as  $[^3\text{H}]\text{Et}_3\text{P}$ . The data in Fig. 9 also demonstrate that efflux of  $[^{195}\text{Au}]$  and  $[^3\text{H}]\text{Et}_3\text{P}$  was temperature dependent. Essentially no radiolabel dissociated from cells at  $4^\circ$ , but at  $37^\circ$  efflux of both  $[^{195}\text{Au}]$  and  $[^3\text{H}]\text{Et}_3\text{P}$  was observed. Efflux was not studied at later time points due to cell lysis. Fractionation studies (Fig. 10, A and B) indicate a redistribution of  $[^{195}\text{Au}]$  and  $[^3\text{H}]\text{Et}_3\text{P}$  from the cytosol to membrane fractions over time. These data suggest

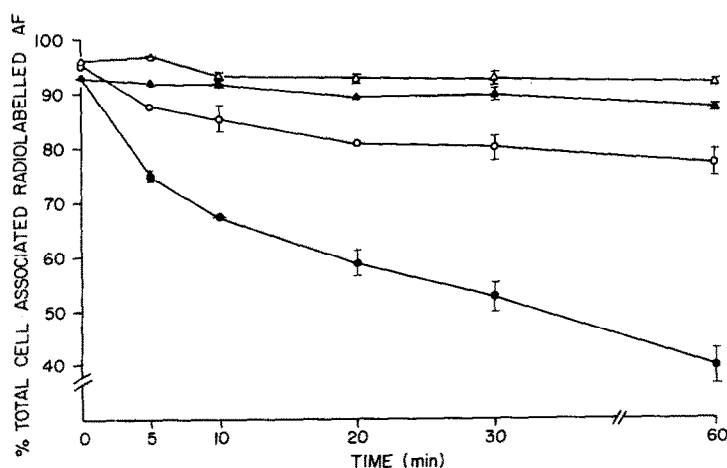


Fig. 9. Efflux of cell-associated radiolabel. Experimental procedures are as described in Materials and Methods. The values shown are means and standard deviations from two separate experiments performed in duplicate. Key: ( $\triangle$ — $\triangle$ )  $4^\circ$ ,  $[^{195}\text{Au}]$ ; ( $\circ$ — $\circ$ )  $37^\circ$ ,  $[^{195}\text{Au}]$ ; ( $\blacktriangle$ — $\blacktriangle$ )  $4^\circ$ ,  $[^3\text{H}]\text{Et}_3\text{P}$ ; and ( $\bullet$ — $\bullet$ )  $37^\circ$ ,  $[^3\text{H}]\text{Et}_3\text{P}$ .

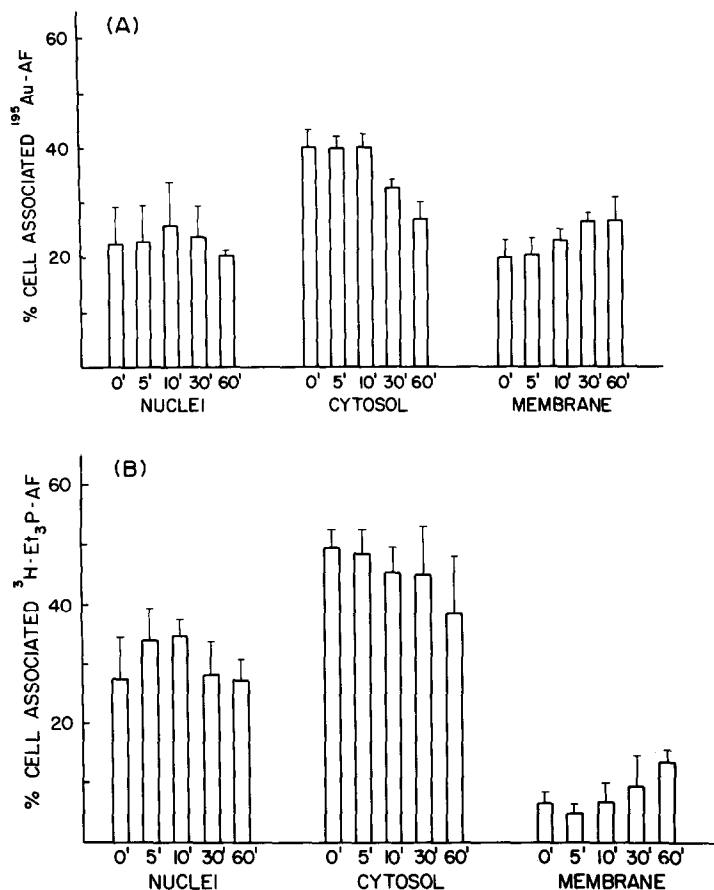


Fig. 10. Subcellular distribution of radiolabel as affected by efflux. Experimental procedures are as described in Materials and Methods. Figure 10A presents data from experiments performed with  $^{195}\text{AuAF}$ ; and 10B from those performed with  $^3\text{H-Et}_3\text{P-AF}$ . The values shown are means and standard deviations from two separate experiments performed in duplicate.

that under non-equilibrium conditions  $^{195}\text{Au}$  and  $^3\text{H-Et}_3\text{P}$  dissociate from cytosolic and/or nuclear binding sites and subsequently reassociate with membrane targets before leaving the cells.

#### DISCUSSION

Figure 11 shows a model for cellular association, distribution, and efflux of auranofin. Cell association (Fig. 11A), or the net cellular accumulation of the drug in the cell pellet, results from the sequential shuttling of the  $\text{Au-Et}_3\text{P}$  or  $\text{Au}$  moieties of the AF molecule between cellular sulfhydryl groups. Initial cell association, the rate-limiting step in the sequential exchange process, occurs because surface membrane-localized thiols successfully compete with TATG for one of the coordinate bonds of the gold. High or low molecular weight extracellular thiols such as albumin or cysteine compete with membrane-localized thiol groups for the TATG ligating site. TATG forms a bond with the gold in auranofin that is stable in the absence of thiol groups but labile to attack by competing thiols.

Support for the reaction sequence proposed for cell association derives from a number of sources.

First, auranofin has been shown to be stable in aqueous medium in the absence of thiols [24]. In the presence of thiols, auranofin readily decomposes [25]. The model predicts that (1) cell association will be temperature dependent, (2) little TATG will associate with the cells or other thiol-containing compounds such as albumin and (3) at least some triethylphosphine should be associated with cells. Cell association was temperature dependent (Fig. 4) and, as predicted, only trace amounts of TATG associated with cells at any time. The small amount of TATG associated with cells was probably a result of TATG partitioning in the lipid of the membranes after ligand exchange. Finally, the phosphine moiety was associated with cells and, at brief time points, the stoichiometry of gold to triethylphosphine associated with the cells was approximately 1:1 (Fig. 3).

The model also predicts that extracellular thiols will compete for auranofin and reduce cell association. While the data in Fig. 6 suggest a significant effect of FCS in inhibiting gold uptake into cells, even in the presence of 10% FCS, which represents a 13-fold excess of extracellular sulfhydryl group to drug, 5% of the  $\text{Au}$  still associated with cells. Under similar experimental conditions with  $\text{B}_{16}$  melanoma

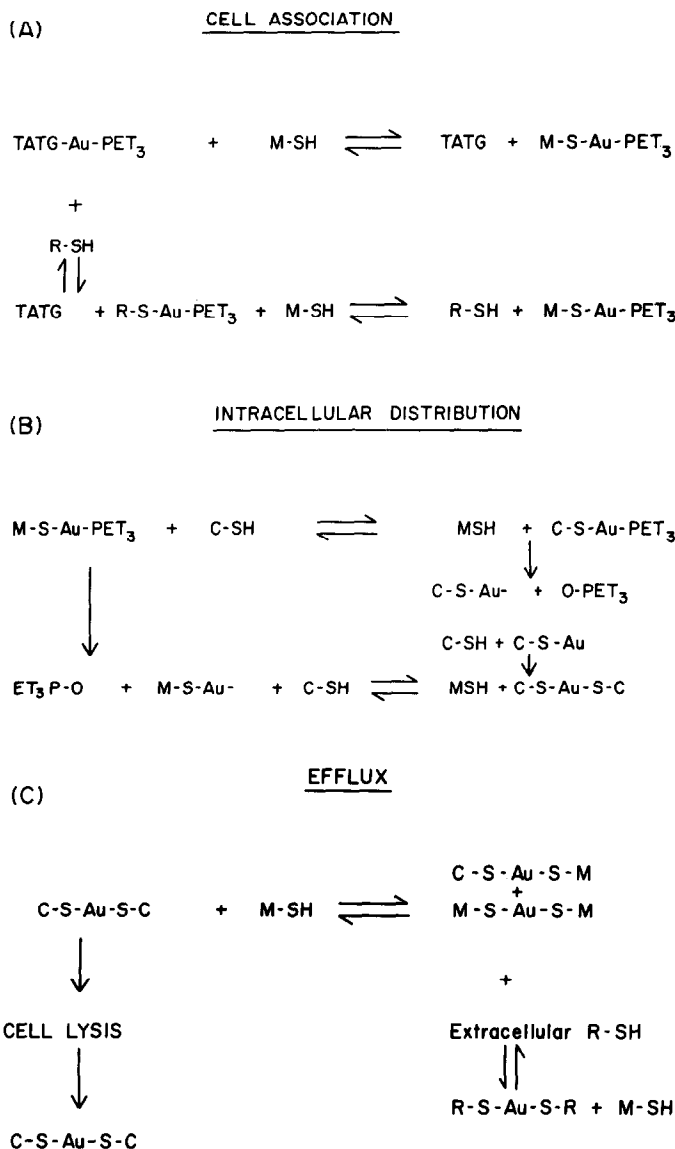


Fig. 11. Model of cell association, intracellular distribution, and efflux of auranofin and metabolites. Panel A describes the process of cell association; panel B, intracellular distribution; and panel C, efflux. Abbreviations: M-SH: membrane localized sulfhydryl groups; R-SH: extracellular sulfhydryl groups; C-SH: cytosolic sulfhydryl groups; Et<sub>3</sub>P: triethylphosphine; and TATG: tetraacetylthioglucose.

cells [18], we have shown that even a greater percentage of protein-associated gold was transferred to cells. These data suggest that gold, ligated to extracellular thiols, exchanges to cellular membrane thiols. However, the contribution of the exchange of Au-associated extracellular thiols to the overall cellular association of Au was small relative to the primary reaction shown at the top of Fig. 11A. Consequently, the addition of FCS or albumin reduced total cellular association of Au relative to FCS or albumin-free medium.

Intracellular distribution of AF (Fig. 11B) results from shuttling of membrane sulfhydryl-bound gold-triethylphosphine to cytosolic sulfhydryl groups. The model suggests that this may occur via two reaction

sequences. The top reaction suggests that cytosolic localized sulfhydryl groups compete for membrane bound gold-triethylphosphine at the former TATG ligation site. Although only a single sulfhydryl exchange is shown, multiple intramembrane ligand exchanges may take place before the gold-triethylphosphine complex becomes associated with cytosolic sulfhydryl groups. Studies with intact erythrocytes and diamide, a sulfhydryl oxidizing agent, also suggest that approximately 80% of membrane protein SH groups are close enough to one another to permit these chemical interactions [26]. Alternatively, oxidative loss of the triethylphosphine moiety in the membrane may precede "shuttling" into the cytoplasm. Support for this step in the reac-



tion sequence derives from several experiments. The model predicts that at short time points gold and triethylphosphine should bind to membranes at a molar ratio of 1:1. Figure 8C shows that this is the case. The model predicts that with time the 1:1 stoichiometry should be altered. This is also shown in Fig. 8C. As cytoplasmically localized gold may derive from both reactions, the stoichiometry of cytoplasmic gold to triethylphosphine is difficult to predict, but it should not be 1:1 (Fig. 8B). Finally, triethylphosphine oxide has been detected in human, rat and dog blood and serum,\* consistent with the notion that oxidative loss of this ligand may occur [27, 28].

Cellular efflux is suggested by the model (Fig. 11C) to be simply the reverse of cell association and intracellular distribution. Figure 9 shows that efflux was time and temperature dependent and occurred at times when essentially no cell lysis was observed. Furthermore, the model predicts that the addition of extracellular sulfhydryl groups during the efflux incubations should increase efflux. Preliminary data demonstrate that this occurred and that the effects were sulfhydryl group concentration dependent.†

Data presented in this study provide the first explanation as to the mechanisms by which the gold in auranofin becomes cell associated. That cellular uptake of the gold in auranofin occurs via a ligand exchange shuttle suggests that initial cellular association is likely to be independent of cellular activity unless the activity alters the exposure of sulfhydryl groups at the cell surface. However, the intracellular distribution and the effects of the gold in auranofin may be dramatically affected by the cell type and cellular activity, since membrane fluidity, the characteristics, concentration and localization of intracellular sulfhydryl groups and repair of membrane damage will play critical roles in determining the fate of the gold in auranofin and its effects.

Data presented here show that the first sites likely to be damaged by auranofin are cellular membranes. Auranofin has been shown to be highly cytotoxic [18, 29–31]. Cell lysis occurs rapidly and is not explained by effects on macromolecular synthesis [18, 32]. Thus, the cytotoxicity and perhaps the chrysotherapeutic effects of auranofin may result from effects on membranes and the membrane activities of target cells.

The data presented confirm and extend the concept that the active moiety in gold-containing antiarthritics is the gold and that the ligands attached to the gold alter pharmacokinetics and intracellular distribution. The model provides a rationale as to how cellular uptake and distribution occur and suggests that the ligand may provide relative selectivity for certain sulfhydryl groups based on relative affinities for gold, lipophilicity, charge and steric factors.

A potentially crucial difference between auranofin and other chrysotherapeutics is the presence of the triethylphosphine group that appears to be displaced only after oxidation to the phosphine oxide. This may result in differences in interactions in membranes as a function of the capacity of various cells to oxidize triethylphosphine and may also represent an additional mechanism of cytotoxicity if cytotoxic free radicals are generated in the process of oxidation of the triethylphosphine moiety.

The sulfhydryl shuttle mechanism proposed differs from traditional concepts of cellular uptake. It is not passive diffusion. Drug molecules do not enter the cell as a function of a concentration gradient. Mirabelli *et al.* [18], using B16 melanoma cells, found that at experimentally measured  $IC_{50}$  concentrations of AF, the cell-associated gold was approximately 100-fold higher than the extracellular concentration of the drug. Nor can it be considered facilitated diffusion or active transport as no specific membrane-localized carrier system is necessary. Our data also suggest that the process does not require ATP as an energy source, since incubations with DNP, at concentrations that were at least 10-fold less than that required to produce cell death but that were within a concentration range reported to inhibit oxidative phosphorylation, had no effect on cellular association. Neither is uptake solely the result of constitutive or stimulus-triggered endocytosis since NaF, an inhibitor of phagocytosis and pinocytosis, was ineffective in preventing association of [ $^{195}Au$ ] from radiolabeled auranofin. Rather, the ligand exchange process simply depends on the chemical reactivities of the drug and cellular sulfhydryl containing components. The proposed mechanism is further strengthened by data showing that [ $^{195}Au$ ] association is inhibited by NEM in a concentration-dependent manner.

That the shuttle mechanism is a generic phenomenon is shown by data in B<sub>16</sub> melanoma cells [18] and by studies in red blood cells.‡ Thus, the *in vivo* localization and the effects of auranofin on the putative target cells, the macrophages, and other cells may be determined to a significant extent by this mechanism and the relative sensitivities of each cell population to gold-sulfhydryl group interactions. Consequently, the model may provide explanations for similarities and differences in effects of various gold compounds and rationales for the synthesis of new gold-containing analogs. Preliminary data observed with triethylphosphine gold chloride demonstrate that the process proposed appears to occur with gold compounds other than auranofin.§ Moreover, any compound capable of interacting with sulfhydryl groups in a similar fashion may undergo an equivalent process. Thus, other metal-containing compounds as well as organic molecules that interact with sulfhydryl groups such as mAMSA [33] may be taken up by cells by this process.

\* Personal communication, cited with the permission of S. Kuo and J. Dent.

† R. Snyder and S. T. Crooke, unpublished results.

‡ Personal communication, cited with permission of B. Hwang and J. Dent.

§ R. Snyder and S. T. Crooke, unpublished results.

**Acknowledgements**—We thank Drs. John Dent and William Johnson for helpful discussions. We also give special thanks to Dr. Lawrence Kruse for excellent critiques and suggestions and to Dr. Richard Heys for making available to us the radiolabeled compounds used in these studies. We thank Ms. Judy Seaman for excellent secretarial assistance.

## REFERENCES

1. G. B. Bluhm, *J. Rheumatol.* **9** (Suppl. 8), 10 (1982).
2. B. M. Sutton, in *Platinum, Gold and Other Metal Chemotherapeutic Agents* (Ed. S. J. Lippard), pp. 356-69. American Chemical Society, Washington, DC (1983).
3. C. F. Shaw, *Inorg. Perspect. Biol. Med.* **2**, 287 (1979).
4. D. J. Sadler, *Structure Bonding* **29**, 171 (1976).
5. H. A. Capell, D. S. Cole, K. K. Manghani and R. W. Morris (Eds.), *Auranofin: Proceedings of a Smith Kline and French International Symposium*. Excerpta Medica, Amsterdam (1983).
6. D. T. Walz, M. J. DiMartino and D. E. Griswold, *Scand. J. Rheumatol.* Suppl. 51, 16 (1984).
7. N. Hanna, M. J. DiMartino, D. E. Griswold and G. Poste, in *Auranofin: Proceedings of a Smith Kline and French International Symposium* (Eds. H. A. Capell, D. S. Cole, K. K. Manghani and R. W. Morris), pp. 60-70. Excerpta Medica, Amsterdam (1983).
8. P. E. Lipsky, *Agents Actions suppl.* **14**, 181 (1984).
9. G. Salmeron and P. E. Lipsky, in *Rheumatology, an Annual Review* (Eds. N. Schattenkirchner and W. Muller), Vol. 8, pp. 63-74. Karger, Basel (1983).
10. G. Salmeron and P. E. Lipsky, *J. Rheumatol.* **9**, (Suppl. 8), 25 (1982).
11. R. J. Coughlan, M. B. Richter and G. S. Panayi, *Clin. Rheumatol.* **3** (Suppl. 1), 25 (1984).
12. K. J. Lawson, C. J. Danpure and D. A. Fyfe, *Biochem. Pharmac.* **26**, 2417 (1977).
13. B. Moeller-Madsen, S. C. Morgensen and G. Dauscher, *Expl molec. Path.* **40**, 148 (1984).
14. C. F. Shaw, H. O. Thompson, P. Witkiewicz, R. W. Satre and K. Siegesmund, *Toxic. appl. Pharmac.* **61**, 349 (1981).
15. F. N. Ghadially, *J. Rheumatol.* **6**, (Suppl. 5), 45 (1979).
16. H. O. Thompson, J. Blaszkak, C. J. Knudson and C. F. Shaw, *Bioinorg. Chem.* **9**, 375 (1978).
17. W. C. Raschke, S. Baird, P. Ralph and I. Nakoinz, *Cell* **15**, 261 (1978).
18. C. K. Mirabelli, R. K. Johnson, C. M. Sung, L. Faucette, K. Muirhead and S. T. Crooke, *Cancer Res.* **45**, 32 (1985).
19. L. B. Chen, I. C. Summerhayes, L. V. Johnson, M. L. Walsh, S. D. Bernal and T. J. Lampidis, *Cold Spring Harb. Symp. Quant. Biol.* **XVI**, 141 (1982).
20. P. G. Heytler, *Meth. Enzym.* **LV**, 462 (1979).
21. R. M. Kaschnitz, Y. Hatefi, P. L. Pedersen and H. P. Morris, *Meth. Enzym.* **LV**, 79 (1979).
22. S. C. Silverstein, R. M. Steinman and Z. A. Cohn, *A. Rev. Biochem.* **46**, 669 (1977).
23. D. H. Brown and W. E. Smith, in *Bioinorganic Chemistry of Gold Coordination Compounds: Proceedings of a Symposium* (Eds. B. M. Sutton and R. G. Franz), pp. 143-56. Smith Kline & French Laboratories, Philadelphia, PA (1981).
24. I. C. Smith, A. Joyce and H. Jarrell, in *Bioinorganic Chemistry of Gold Coordination Compounds: Proceedings of a Symposium* (Eds. B. M. Sutton and R. G. Franz), pp. 47-52. Smith Kline & French Laboratories, Philadelphia, PA (1981).
25. C. F. Shaw in *Bioinorganic Chemistry of Gold Coordination Compounds: Proceedings of a Symposium* (Eds. B. M. Sutton and R. G. Franz), pp. 98-123. Smith Kline & French Laboratories, Philadelphia, PA (1981).
26. C. W. M. Haest, D. Kamp, G. Plasa and B. Deuticke, *Biochim. biophys. Acta* **469**, 226 (1977).
27. A. P. Intoccia, T. L. Flanagan, D. T. Walz, L. Gutzait, J. E. Swagdis, J. Flagiello, B. Hwang, R. H. Dewey and H. Noguchi, *J. Rheumatol.* **9**, (Suppl. 8), 90 (1982).
28. M. C. Grootveld, M. T. Razi and P. J. Sadler, *Clin. Rheumatol.* **3** (Suppl. 1), 5 (1984).
29. T. M. Simon, D. H. Kunishima, G. H. Vibert and A. Lorber, *J. Rheumatol.* **6** (Suppl. 5), 91 (1979).
30. T. M. Simon, D. H. Kunishima, G. H. Vibert and A. Lorber, *Cancer Res.* **41**, 94 (1981).
31. C. K. Mirabelli and S. T. Crooke in *Auranofin: Proceedings of a Smith Kline and French International Symposium* (Eds. H. A. Capell, D. S. Cole, K. K. Manghani and R. W. Morris), pp. 17-31. Excerpta Medica, Amsterdam (1983).
32. H. S. Allaudeen, R. M. Snyder, M. H. Whitman and S. T. Crooke, *Biochem. Pharmac.* **34**, 3243 (1985).
33. A. Wong and S. T. Crooke, *Biochem. Pharmac.* **34**, 3265 (1985).